Langmuir

Article

pubs.acs.org/Langmuir

Electrospun Nanofibrous Membranes Surface-Decorated with Silver Nanoparticles as Flexible and Active/Sensitive Substrates for Surface-Enhanced Raman Scattering

Lifeng Zhang,[†,§,∥] Xiao Gong,[‡,§] Ying Bao,[‡] Yong Zhao,[†] Min Xi,[†] Chaoyang Jiang,*[,‡] and Hao Fong*[,†]

[†]Department of Chemistry, South Dakota School of Mines and Technology, Rapid City, South Dakota 57701, United States

[‡]Department of Chemistry, University of South Dakota, Vermillion, South Dakota 57069, United States

Supporting Information

ABSTRACT: The development of novel nanomaterials with well-controlled morphologies/structures to achieve excellent activities/sensitivities in surface-enhanced Raman scattering (SERS) is crucial in advancing the high-performance SERS detections of chemical and biological species. In this study, amidoxime surface-functionalized polyacrylonitrile (ASFPAN) nanofibrous membranes surface-decorated with silver nanoparticles (Ag NPs) were prepared via the technique of electrospinning followed by the method of seed-mediated electroless plating. High SERS activities/sensitivities were observed from the ASFPAN-Ag NPs nanofibrous membranes, while the density and size of Ag NPs had an important impact on the SERS activity/sensitivity. The results confirmed that the enhancement of Raman signals is due to the presence of hot spots between/among Ag NPs on the nanofiber surfaces. Electrospun nanofibrous membranes surface-decorated with Ag NPs were mechanical flexible/resilient and could be used as highly active/sensitive SERS substrates for a broad range of applications.

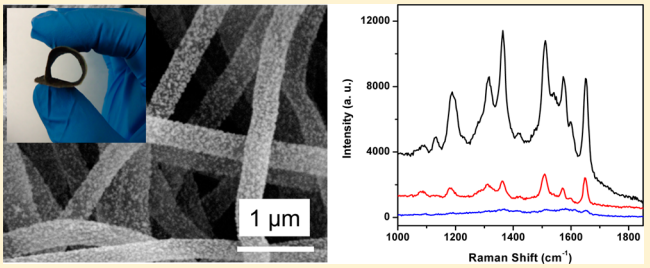

1. INTRODUCTION

Surface-enhanced Raman scattering (SERS) has been widely studied for ultrasensitive chemical and biological detections, because it can provide the molecule-level information of analytes adsorbed on SERS-active substrates.[1−4] Noble metal nanostructures, particularly those made of Au and Ag, have shown excellent SERS activities due to their unique characteristics of localized surface plasmon resonances (SPRs).[5−8] The nanoscale gaps in these materials, known as the Raman "hot spots", can dramatically enhance the local electromagnetic field, resulting in enormously strong Raman enhancement when molecules of analytes are trapped inside and/or close enough.[9,10] Research efforts have revealed that the aggregations of Au/Ag nanoparticles would exhibit much stronger SERS enhancements as compared to isolated/individual ones due to the collective SPRs with interparticle plasmon coupling.[11−15] Hence, there is a growing interest to design novel substrates with desired aggregations to improve SERS activities, for example, the substrates made of three-dimensional hierarchical aggregations of Au/Ag.[16,17] To further facilitate and broaden the SERS application, it is important to explore facile, cost-effective, scalable, and reproducible approaches for the preparation of nanostructured SERS substrates with controlled morphologies and structures of nanoparticle aggregations to achieve ultrahigh SERS activities/sensitivities.

The nanomaterials-processing technique of electrospinning provides a versatile approach for the convenient fabrication of fibers with diameters typically ranging from tens to hundreds of nanometers (i.e., electrospun nanofibers).[18,19] The membranes made of electrospun polymer nanofibers are flexible, cost-effective, and relatively easy to be assembled/processed for a variety of applications.[20,21] Recently, there have been several reports on the fabrication of electrospun nanofibers containing metal nanostructures, and SERS activities/enhancements of the resulting hierarchical nanofibers (and/or nanofibrous membranes) have been explored.[22−29] For example, Yu and co-workers embedded Ag nanoparticles in electrospun poly(vinyl alcohol) nanofibers, and high SERS sensitivity was detected;[24] similarly, Au nanoparticles/nanorods can also be assembled inside electrospun polymer nanofibers for SERS applications.[25,26] As compared to the common SERS substrates, such as microspheres decorated with silver nanostructures,[30] electrospun nanofiber-based SERS substrates have several advantages such as being suitable for surface modification during sample preparation, mechanical resilience, and can be freestanding and three-dimensionally porous for analytes to easily access. Hence, there is a great chance to develop flexible SERS substrates with outstanding SERS performance using the electrospun nanofibers. However, the SERS-active metal nanostructures reported previously were mostly embedded/encapsulated in polymer matrixes; thus, the molecules of

Received: July 10, 2012
Revised: September 8, 2012
Published: September 13, 2012

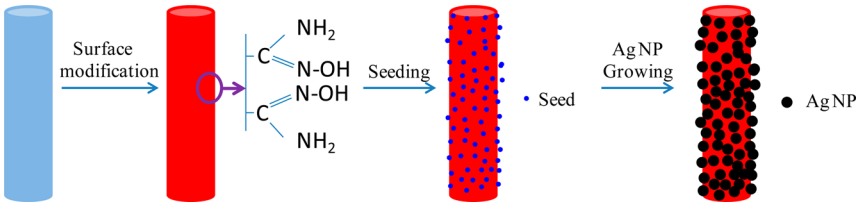

Figure 1. A schematic diagram showing the preparation of SERS-active electrospun nanofibers surface-decorated with Ag NPs.

analytes have to diffuse/permeate into nanofibers to access these metal nanostructures.

Metal nanostructures that attached to electrospun nanofibers can adsorb analytes directly on their surfaces, leading to superior SERS sensitivity. Such hierarchical SERS substrates can be prepared by attaching metal nanostructures onto electrospun nanofibers via methods such as drop-casting, electroplating, sputter-coating, chemical reduction, and electroless plating.[27,28,31−35] These nanofibrous substrates possess desired properties in thermal diffusivity, conductivity, electrocatalytic activity, and SERS sensitivity. For example, He and coworkers prepared porous silver nanotubes through a combination of metal evaporation and plasma etching methods and explored their SERS enhancements;[26] Singamaneni and coworkers used the drop-cast method and obtained oriented Au nanorods on electrospun nanofibers with high SERS sensitivity.[28] As compared to the methods of evaporation and/or postsynthesis nanoparticle attachment, the method of direct growth of metal nanostructures onto electrospun nanofibers via wet-chemistry reactions has several advantages due to the versatility and capability for precise control of the size, shape, density, and aggregation of metal nanostructures. Nevertheless, to the best of our knowledge, there has been no reported study on SERS activities of the electrospun nanofibrous substrates surface-attached/decorated with metal nanoparticles made from direct growth.

In this Article, we report a new approach to prepare flexible and highly sensitive SERS substrates via directly growing silver nanoparticles (Ag NPs) on electrospun polymer nanofibers. The most favorable morphologies/structures of Ag NPs on the surface of electrospun nanofibers were identified on the basis of SERS performance evaluation, as well as the nanoscale structural characterizations. The formation of nanoscale interparticle junctions (i.e., the Raman "hot spots"), together with high surface area and porosity of the electrospun nanofibrous membranes, rendered the high SERS sensitivities. This study revealed a simple while efficient approach to prepare highly sensitive nanofibrous membranes for a variety of SERS applications.

2. EXPERIMENTAL SECTION

2.1. Materials. The polyacrylonitrile (PAN) used in this study was the PAN microfibers provided by the Courtaulds, Ltd. (Nottingham, UK). Acetone, *N*,*N*-dimethylformamide (DMF), hydroxylamine (NH_2OH), silver nitrate ($AgNO_3$), palladium chloride ($PdCl_2$), tin chloride ($SnCl_2$), potassium hydroxide (KOH), and ammonium hydroxide (NH_4OH) were purchased from the Sigma-Aldrich Chemical Co. (St. Louis, MO) and used without further purification.

2.2. Preparation of Electrospun Nanofibrous Membranes. PAN microfibers were first dissolved in DMF to make a 14 wt % solution. The solution was then filled in a 30 mL BD Luer-Lok tip plastic syringe having an 18 gauge stainless-steel needle with a 90° blunt end. The electrospinning setup included a high voltage power supply purchased from Gamma High Voltage Research Inc. (Ormond Beach, FL) and a laboratory-made roller with a diameter of 10 in. The roller was placed 9 in. away from the tip of needle. During electrospinning, a positive high voltage of 20 kV was applied to the needle, and a solution feed rate of 1.1 mL/h was maintained using a syringe pump purchased from KD Scientific Inc. (Holliston, MA). PAN nanofibers were collected as overlaid membranes on electrically grounded aluminum foil that covered the roller. After being electrospun, the nanofibrous membranes were separated from the aluminum foil for further treatments and characterizations.

2.3. Growth of Ag NPs on Electrospun Nanofibrous Membranes. Prior to the growth of Ag NPs, as-electrospun PAN nanofibrous membranes were first treated in 1 M NH_2OH aqueous solution at 70 °C for 5 min; some −C≡N groups on the surface of nanofibers reacted with NH_2OH, leading to the formation of $-C(NH_2)=N-OH$ groups. After the treatment, the obtained amidoxime surface-functionalized PAN (ASFPAN) nanofibrous membranes were thoroughly rinsed in distilled water and dried before the growth of Ag NPs.

Subsequently, the surface of ASFPAN nanofibrous membranes was activated before the electroless deposition of Ag NPs. Herein, a typical $SnCl_2/PdCl_2$ method was applied to introduce palladium seeds on nanofiber surface.[36] During the seeding process, an ASFPAN nanofibrous membrane was first immersed in 3.0 mM $SnCl_2$ aqueous solution for 30 min and then in 3.0 mM $PdCl_2$ solution for 10 min. This process would introduce Pd seeds on the ASFPAN nanofibers, and the seeds would become active sites for the following nucleation and growth of Ag NPs.

The electroless plating of Ag NPs onto the activated ASFPAN nanofibrous membranes was conducted using the Tollen's reagent consisting of two parts. The first part was prepared by addition of 15 M NH_4OH aqueous solution dropwise into 30 mL of 0.1 M $AgNO_3$ aqueous solution until the brown precipitate disappeared under constant stirring; after that, 15 mL of 0.8 M KOH aqueous solution was added to the system, resulting in a black precipitate. An additional NH_4OH was then added dropwise until the system became clear and colorless again. The second part was 3 mL of 0.25 M dextrose aqueous solution. Both parts were subsequently mixed together for 20 s under constant stirring. Finally, the surface activated ASFPAN nanofibrous membranes were immersed in Tollen's reagent for electroless plating. After several minutes of the reaction, the nanofibrous membranes were thoroughly rinsed with distilled water and dried in air before morphological/structural characterizations and SERS evaluations.

2.4. Morphological and Structural Characterizations. ASFPAN nanofibrous membranes surface-decorated with Ag NPs were characterized with several microscopic and spectroscopic methods. A Zeiss Supra 40VP field-emission scanning electron microscope (SEM) was employed to examine morphologies of the prepared membranes. The size, shape, and density of Ag NPs were characterized on a JEOL JEM-2100 transmission electron microscope (TEM) and a Tecnai Spirit G2 Twin TEM. X-ray diffraction (XRD) patterns were acquired from a Rigaku Ultima Plus X-ray diffractometer operating at 40 kV and 90 mA with the Cu K_α radiation (wavelength λ = 0.154 nm). UV−vis reflectance spectra were acquired from a Leica optical microscope with a Craig point-shot spectrometer. The ASFPAN nanofibrous membranes without silver coating were used for background correction.

2.5. SERS Evaluations. SERS spectra and confocal Raman mappings were acquired from an Aramis confocal microscope (Horiba Jobin Yvon, Edison, NJ) equipped with a diode-pump solid state (DSPP) laser (532 nm). The laser beam with an intensity of 0.4 mW

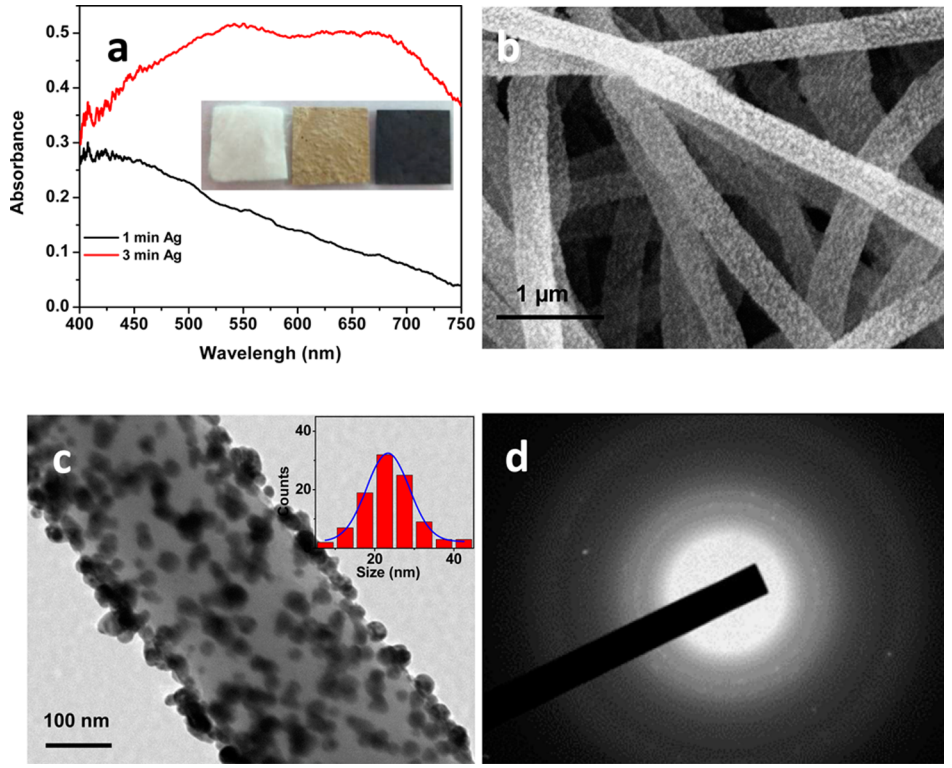

Figure 2. (a) Reflectance spectra of the ASFPAN nanofibrous membranes with the deposition of Ag NPs for 1 and 3 min. Photographs of three nanofibrous membranes (PAN, ASFPAN, and ASFPAN-Ag NPs) are shown in the inset. Representative SEM image (b) and TEM image (c) of ASFPAN nanofibers after the process of electroless plating for 3 min. Inset in (c) shows the size distribution of Ag NPs. The image (d) shows the select-area electron diffraction pattern of Figure 1c.

(unless specified otherwise) was focused using a 50× objective (NA 0.75) onto the nanofibrous membranes on glass slides, which were mounted onto a 200 × 200 × 200 μm piezo scanner. The Raman signals were collected with the same objective under a 180° backscattering configuration and passed through an edge filter into a monochromator and electric-cooled charge-coupled devices (CCD) camera. The Raman spectra were collected for 1 s at each location, and Raman maps were obtained on the same confocal microscope according to a reported method.[37]

3. RESULTS AND DISCUSSION

3.1. Preparation and Characterization of Nanofibrous Membranes Surface-Decorated with Ag NPs. Surface modification and activation of electrospun nanofibers can significantly influence the deposition of Ag NPs on these nanofibers. Figure 1 is a schematic diagram showing the steps on how to fabricate SERS-active ASFPAN nanofibrous membranes surface-decorated with silver nanoparticles (ASFPAN-Ag NPs). PAN nanofibers were first prepared via electrospinning. The surface of PAN nanofibers was then modified through amidoxime ($-C(NH_2)=N-OH$) surface functionalization. Amidoximation of PAN nanofibers resulted in the formation of $-C(NH_2)=N-OH$ groups on the fiber surfaces, leading to considerable increase of hydrophilicity for the nanofibrous membranes. FTIR and SEM have been used to characterize the functionalized nanofibers, as was reported in our recent article.[38]

After that, the seeding process was carried out with a $SnCl_2$/$PdCl_2$ method, and finally the Ag NPs with different size and density were grown on the surface of nanofibers. The amidoxime group is a coordinating/chelating group with high affinity to metal ions.[38,39] Therefore, the ASFPAN nanofibers were in favor of the following treatments of seeding and electroless plating. The seeding process (represented by the following reaction) can facilitate the uniform nucleation and fast growth of Ag NPs.

$$SnCl_2 + PdCl_2 \rightarrow SnCl_4 + Pd$$

Because of the catalytic properties, the palladium seeds on nanofiber surface acted as active sites for reaction of silver ions and dextrose molecules and eventually became the sites for nucleation of Ag NPs.[40] The reduction of silver ions into elemental silver is well-known; in the reaction, silver ions accept electrons and are reduced to silver atoms; dextrose molecules (D−CHO) donate electrons and are oxidized to species containing carboxyl/carboxylate, as shown in the following equation:

$$D-CHO + 2[Ag(NH_3)_2]^+ + 3OH^- \rightarrow 2Ag + D-COO^- + 4NH_3 + 2H_2O$$

During electroless deposition of Ag NPs on the surface of ASFPAN nanofibers, the size and density of Ag NPs can be adjusted via growing time, solution stirring, temperature, and other experimental conditions.

Optical and structural characterizations were carried out on electrospun ASFPAN nanofibrous membranes surface-decorated with Ag NPs. The inset of Figure 2a shows the photographs of ASFPAN nanofibrous membranes before and after the deposition of Ag NPs. It was observed that the color of PAN nanofibrous membranes changed from white to yellow and then gray after the process of electroless plating, indicating the deposition of Ag NPs on fiber surface. UV−vis reflectance

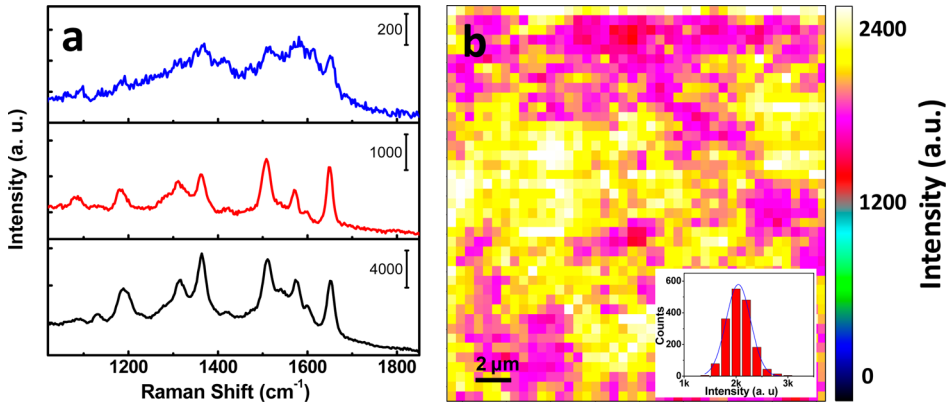

Figure 3. (a) Typical SERS spectra of the ASFPAN nanofibrous membranes after the deposition of Ag NPs for 3 min and treated with R6G solutions with different concentrations (top to bottom: 10, 100, and 1000 ppb). (b) Confocal Raman map from the ASFPAN-Ag NPs nanofibrous membrane, and the inset is a histogram of intensity.

spectroscopy (UV-RS) was also conducted to further confirm the existence of Ag NPs. As shown in Figure 2a, the reflectance spectrum of ASFPAN with Ag NPs possessed two distinguishable absorptions centered at 544 and 666 nm, which did not exist in the spectrum of the nanofibers before the deposition of Ag NPs. The peak centered at 544 nm could be attributed to the absorption of Ag NPs due to silver's unique SPRs, as being reported by others.[41] The second peak centered at 666 nm could be assigned to collective SPRs originated from interparticle interactions in the aggregations of Ag NPs;[24] it might also be attributed to the partial oxidation of Ag NPs.[42] In either case, the attachment of Ag NPs onto ASFPAN nanofibers could be confirmed by the color change and by the characteristic absorption peaks in visible spectra.

The morphological/structural characterizations of ASFPAN nanofibrous membranes after the deposition of Ag NPs for 3 min were conducted with both SEM and TEM. A typical SEM micrograph of the ASFPAN nanofibrous membranes after the deposition Ag NPs is shown in Figure 2b. Uniform nanofibers with an average diameter of ~300 nm could be clearly observed in the SEM image. Furthermore, many nanoscale particles could be observed on the surface of nanofibers; these bright particles were Ag NPs because silver could scatter more electrons than polymer nanofibers. From the SEM images, it was concluded that the Ag NPs were randomly distributed on the surface of nanofibers. It is noteworthy that the Ag NPs, at the macroscale, were uniformly attached to the nanofibers. This was substantially different as compared to the morphology of Ag NPs grown on the PAN nanofibers, as shown in Figure S1 in the Supporting Information.

The sizes of Ag NPs were then determined via the TEM investigation. TEM results provided further structural information on these nanoparticles and nanofibers. A typical TEM image is shown in Figure 2c, in which numerous Ag NPs were attached onto an ASFPAN nanofiber. The Ag NPs were roughly spherical in shape and were randomly distributed on the surface of the nanofiber with a moderate density. More TEM micrographs are shown in Figure S2, and similar spherical shapes were observed. The density of Ag NPs obtained from the TEM image was consistent with that obtained from the SEM results. The size distribution of Ag NPs is shown in the inset of Figure 2c, which indicated a normal distribution with an average of 23.3 ± 5.3 nm. To further confirm the presence of Ag NPs, the select-area electron diffraction (SAED) was carried out on ASFPAN-Ag NPs nanofibers, and a typical SAED pattern is shown in Figure 2d. The diffraction dots/spots originated from silver crystals could be clearly identified, while the ring-like diffraction pattern indicated that the Ag NPs were randomly attached on the surface of ASFPAN nanofibers without particular orientation.

3.2. SERS Evaluation of Nanofibrous Membranes Surface-Decorated with Ag NPs. One of the most exciting research topics on the nanoscale silver materials is the activity/sensitivity in SERS applications. Silver nanostructures have been intensively studied to advance the knowledge on the relationship between structure and SERS property and to fabricate SERS-active substrates with high degree of Raman enhancement. The SERS activity/sensitivity of ASFPAN-Ag NPs nanofibrous membranes was studied by using Rhodamine 6G (R6G) as the probe molecule. Figure 3a showed representative R6G SERS spectra from the ASFPAN-Ag NPs nanofibrous membranes that were treated with R6G solutions having concentrations of 10, 100, and 1000 ppb, respectively. The SERS signals were clear when the R6G concentration was 100 ppb or higher. Albeit the SERS intensity decreased with the decrease of R6G concentration, the SERS signals were still identifiable even with 10 ppb R6G solution. The Raman peaks centered at 1096, 1183, 1310, 1362, 1508, 1572, and 1650 cm^{-1} appeared in the SERS spectra, which were consistent with the Raman signals of the adsorbed R6G molecules.[43] The capability of sensing R6G at the 10 ppb concentration made the ASFPAN-Ag NPs nanofibrous membranes very promising as SERS-active substrates for trace chemical detections.

With the confirmed SERS activity/sensitivity of these ASFPAN-Ag NPs nanofibrous membranes, it is extremely important to evaluate their uniformity because having a uniform SERS-active substrate is crucial for a reliable/reproducible SERS measurement. Confocal Raman mappings were conducted on the ASFPAN-Ag NPs nanofibrous membranes to examine the SERS performance. Figure 3b is a typical Raman map of an ASFPAN-Ag NPs nanofibrous membrane with an area of 20 × 20 μm^2, where intensities of the Raman peaks of R6G in the range of 1440−1700 cm^{-1} could be visualized. The map indicated that the Raman intensities were around 2000 counts, and strong Raman signals could be obtained from any location across the examined area. The inset in Figure 3b showed a histogram of SERS intensity. A Gaussian curve was applied to fit the histogram, indicating a normal distribution of SERS intensities in the area of interest. The Gaussian fitting gave an average SERS intensity of 2044 ±

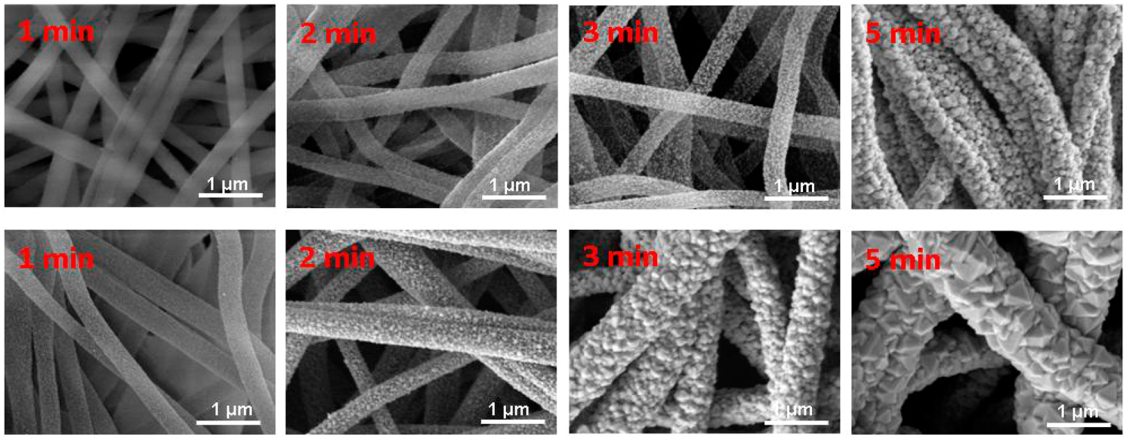

Figure 4. Representative SEM micrographs of ASFPAN-Ag NPs nanofibrous membranes with Ag NPs grown under the conditions of nonstirring (top) and stirring (bottom).

237 counts with a relatively standard deviation of ~10% across the entire area. This was an exciting uniformity, because the area of examination was quite large. Moreover, we believed that some of the intensity variations were associated with the focus issue due to uneven surface of nanofibrous membranes.

The SERS intensity of R6G molecules as a function of the concentration of R6G solution during the sample preparation was studied in detail. ASFPAN-Ag NPs nanofibrous membranes were treated with a series of R6G solutions at the concentrations of 10, 100, 250, 500, 750, and 1000 ppb, respectively. For each sample, several confocal Raman maps were obtained, and the histograms of SERS intensity were plotted and analyzed. Figure S3a showed the dependence of SERS intensity on R6G concentration, which indicated that the SERS intensity first increased substantially with the increase of R6G concentration; after the R6G concentration reached 250 ppb, the SERS intensity increased moderately with the increase of R6G concentration. This could be explained by the saturation of R6G molecules on the surface of ASFPAN-Ag NPs nanofibers. The acquired concentration-dependent results were similar to those in literature.[43] The SERS enhancement factors of R6G on the nanofibrous membranes were estimated, as shown in the concentration-dependent plot (Figure S3b). Additionally, the SERS enhancement factor on the nanofibrous membranes was conducted by using nonfluorescent 4-mercaptobenzoic acid (4-MBA) as the Raman probe. An enhancement factor of 4.8×10^5 was obtained on the basis of the intensity of the band centered at 1070 cm^{-1} in the 4-MBA Raman spectra.

3.3. Tuning the Growth of Ag NPs and Their SERS Activity/Sensitivity. The size, shape, and aggregation of Ag NPs play an important role in determining the SERS activity/sensitivity of ASFPAN-Ag NPs nanofibrous membranes. A series of nanofibrous membranes were prepared by changing the reaction time and stirring condition during the electroless plating deposition of Ag NPs. In one case, the deposition of Ag NPs was carried out by simply immersing the nanofibrous membranes into the solutions, and the solutions were not stirred during the process. Representative SEM micrographs of the resulting membranes with various time periods (ranging from 1 to 5 min) for growing Ag NPs are shown in Figure 4. When the deposition time was 1 min, Ag NPs were hard to identify on the nanofibers. The sample with deposition time of 2 min clearly showed numerous Ag NPs distributed on the surface of nanofibers due to heterogeneous nucleation from catalytically active Pd seeds.[40] Our results indicated that the electroless plating of silver occurred in a form of island growth on the nanofiber surface at this stage. SEM study revealed that the Ag NPs tended to grow in the shape of sphere or ellipsoid. The process of electroless plating would continue the deposition of silver onto already formed Ag NPs, showing the size acceleration of Ag NPs with extended growing time. With further prolonging of the deposition time, the Ag NPs grew larger, and the gap distances between Ag NPs would be reduced. After deposition for 5 min, the particle size could be as large as several hundred nanometers. If the deposition time was too long, the Ag NPs would form polyhedral structures and the particles tended to grow together; this would result in the reduction of the number of interparticle gaps.

It is noteworthy that the stirring of solution during the electroless plating process would lead to faster growth of Ag NPs. As shown in Figure 4, Ag NPs could be clearly observed on the surface of nanofibers upon 1 min electroless plating under stirring condition. The size of these nanoparticles grew much faster than those under nonstirring conditions. After a 5 min electroless plating process, silver particles with sizes of a few micrometers could be observed with distinct crystal facets and polyhedral structures. TEM micrographs of these large particles are also shown in Figure S4, and these crystal facets can be clearly observed. The average sizes of Ag NPs as well as the diameters of ASFPAN nanofibers surface-decorated with Ag NPs were obtained by measuring tens of particles and fibers in the TEM micrographs, and the results are listed in Table 1. The

Table 1. Average Sizes of Ag NPs on the Surface of ASFPAN Nanofibers and the Average Diameters of ASFPAN Nanofibers Surface-Decorated with Ag NPs

	under the condition of nonstirring		under the condition of stirring	
growing time (min)	average size of Ag NPs (nm)	average diameter of nanofibers (nm)	average size of Ag NPs (nm)	average diameter of nanofibers (nm)
1	9.3 ± 1.5	305.5 ± 28.4	11.1 ± 2.0	332.8 ± 74.0
2	19.7 ± 1.9	322.8 ± 47.1	29.3 ± 7.5	382.0 ± 58.1
3	23.4 ± 6.8	324.4 ± 44.7	81.4 ± 5.7	513.8 ± 116.0
5	23.8 ± 4.0	337.5 ± 55.9	108.4 ± 8.6	533.7 ± 57.5

dx.doi.org/10.1021/la302779q | *Langmuir* 2012, 28, 14433−14440

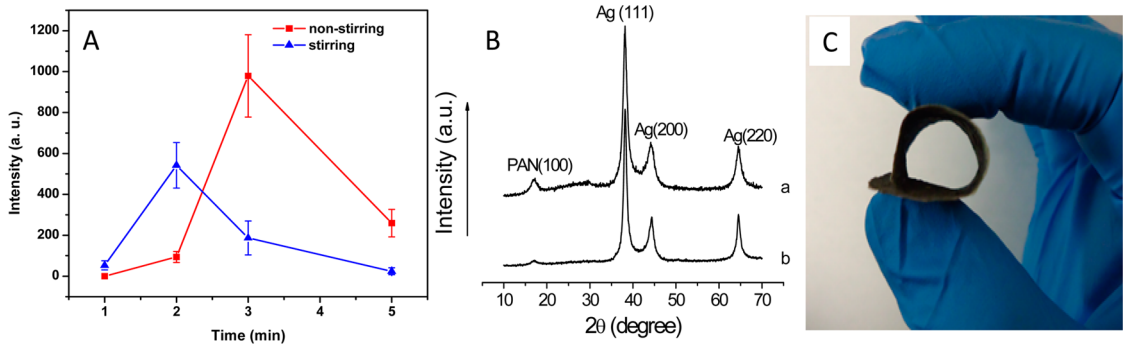

Figure 5. (A) Raman map intensity of ASFPAN-Ag NPs nanofibrous membranes treated with 1 ppm R6G solutions as a function of growing time of Ag NPs (laser power was 0.17 mW); (B) XRD pattern of the ASFPAN-Ag NPs nanofibrous membranes with Ag NPs being grown for 3 min under the condition of nonstirring (a) and being grown for 2 min under the condition of stirring (b); and (C) photograph depicts the excellent mechanical flexibility/resilience of a ASFPAN-Ag NPs nanofibrous membrane.

fast growth of Ag NPs under stirring condition was due to the stirring-induced diffusion rate increase of the silver ions and dextrose molecules to the growth sites on the surface of the nanofibers.

The size, shape, and density of Ag NPs have a significant impact on SERS performance of the nanofibrous membranes. Raman mappings of a series of ASFPAN-Ag NPs nanofibrous membranes were systematically studied for their SERS activities/sensitivities. The results shown in Figure 5a are the average Raman intensities as a function of electroless plating time for ASFPAN-Ag NPs nanofibrous membranes prepared under the conditions of both stirring and nonstirring. The strongest Raman signals were obtained on the nanofibrous membrane with 3 min deposition time under nonstirring condition, and these results were consistent with SEM investigations. As compared to other samples, Ag NPs that were grown for 3 min under nonstirring condition have the appropriate interparticle gap, suitable for the generation of Raman "hot spots". For the samples that were prepared under stirring condition, the maximum SERS sensitivity was observed from the sample with 2 min electroless plating time, and this was consistent with the expectation based upon the consideration of the accelerated growth of Ag NPs due to stirring. For the substrates with the micrometer-scaled silver particle, the SERS activity was too weak to be detected. Such results once again confirmed the importance of interparticle gaps for the generation of Raman "hot spots".

Additional characterizations were conducted on the nanofibrous membranes that gave the best SERS performance in their series. TEM results showed that the average size of Ag NPs in the nonstirring samples (3 min) was ~23 nm. The Ag NPs in the stirring samples were slightly larger (~30 nm). Whereas a direct comparison for SERS activity and particle size between these two nanofibrous substrates was not justifiable due to the lack of identical nanoparticle density and packing morphology, it was still possible to conclude that the SERS activity/sensitivity could be tuned by the properties of ASFPAN-Ag NPs nanofibrous membranes (such as the size and density of Ag NPs). Herein, the size difference of Ag NPs was also confirmed by XRD patterns (Figure 5b). Under both stirring and nonstirring conditions, diffraction peaks centered at 2θ angles of 38.2°, 44.2°, and 64.5° were observed, which could be assigned to (111), (200), and (220) crystallographic planes of the cubic crystal structure of silver metal, respectively.[44] A weak peak centered at 17.0° could be attributed to (100) crystallographic plane in PAN.[39] The XRD peaks from the nanofibrous membranes with 2 min deposition time under stirring condition are slightly narrower than those of the membranes with 3 min deposition time under nonstirring condition, indicating slightly larger silver crystalline domains in the former sample.

It is noteworthy that all of the ASFPAN-Ag NPs nanofibrous membranes possessed excellent mechanical flexibility/resilience. Although decorated with Ag NPs, these nanofibrous membranes could still be folded into a hollow cylinder (as shown in Figure 5c). This desired mechanical flexibility/resilience ensured that these hierarchical nanofibrous membranes could efficiently collect trace amounts of samples, an overlooked factor that was critical for SERS applications in practice.[45] Furthermore, the flexible SERS-active membrane could be tailored into any shape, which would be extremely useful for mobile SERS applications.

4. CONCLUSION

A simple approach has been studied to prepare flexible and highly active/sensitive SERS substrates by electroless plating of Ag NPs on the surface of electrospun nanofibers via the seed-mediated growth process. Randomly distributed Ag NPs with controllable size and density were deposited on ASFPAN nanofibrous membranes. High SERS activities/sensitivities from Ag NPs on the surface of ASFPAN nanofibers were identified using a confocal Raman mapping method. The density and size of Ag NPs, which had an important impact on SERS activity/sensitivity, could be controlled by reaction time and stirring condition. The ASFPAN nanofibrous membranes surface-decorated with Ag NPs were mechanically flexible/resilient and had great potential as highly sensitive SERS substrates for a broad range of applications.

■ ASSOCIATED CONTENT

Supporting Information

Additional figures and experimental details. This material is available free of charge via the Internet at http://pubs.acs.org.

■ AUTHOR INFORMATION

Corresponding Author

*Tel.: (605) 677-6250 (C.J.), (605) 394-1229 (H.F.). Fax: (605) 677-6397 (C.J.), (605) 394-1232 (H.F.). E-mail: chaoyang.jiang@usd.edu (C.J.), hao.fong@sdsmt.edu (H.F.).

Present Address
[‖]Joint School of Nanoscience and Nanoengineering, North Carolina A&T State University and the University of North Carolina at Greensboro, Greensboro, North Carolina 27401, United States.

Author Contributions
[§]These authors contributed equally.

Notes
The authors declare no competing financial interest.

■ ACKNOWLEDGMENTS

This research was supported by the NSF (Grant nos.: EPS-0903804 and DGE-0903685), NASA (cooperative agreement number: NNX10AN34A), and the State of South Dakota. L.Z. and H.F. also acknowledge the Nelson Research Grant at South Dakota School of Mines and Technology (Grant no.: 03284). We are grateful to Ms. L. Tian from Washington University in St. Louis for her help in UV−vis measurements. TEM studies were partially conducted on the instrument funded by the NSF CHE-0840507 grant.

■ REFERENCES

(1) Nie, S. M.; Emery, S. R. Probing Single Molecules and Single Nanoparticles by Surface-Enhanced Raman Scattering. *Science* **1997**, *275*, 1102−1106.
(2) Camden, J. P.; Dieringer, J. A.; Wang, Y. M.; Masiello, D. J.; Marks, L. D.; Schatz, G. C.; Van Duyne, R. P. Probing the Structure of Single-Molecule Surface-Enhanced Raman Scattering Hot Spots. *J. Am. Chem. Soc.* **2008**, *130*, 12616−12617.
(3) Kleinman, S. L.; Ringe, E.; Valley, N.; Wustholz, K. L.; Phillips, E.; Scheidt, K. A.; Schatz, G. C.; Van Duyne, R. P. Single-Molecule Surface-Enhanced Raman Spectroscopy of Crystal Violet Isotopologues: Theory and Experiment. *J. Am. Chem. Soc.* **2011**, *133*, 4115−4122.
(4) Gong, X.; Bao, Y.; Qiu, C.; Jiang, C. Individual Nanostructured Materials: Fabrication and Surface-Enhanced Raman Scattering. *Chem. Commun.* **2012**, *48*, 7003−7018.
(5) Liang, H. Y.; Li, Z. P.; Wang, W. Z.; Wu, Y. S.; Xu, H. X. Highly Surface-Roughened "Flower-Like" Silver Nanoparticles for Extremely Sensitive Substrates of Surface-Enhanced Raman Scattering. *Adv. Mater.* **2009**, *21*, 4614−4618.
(6) Lu, Y.; Liu, G. L.; Lee, L. P. High-Density Silver Nanoparticle Film with Temperature-Controllable Interparticle Spacing for a Tunable Surface Enhanced Raman Scattering Substrate. *Nano Lett.* **2005**, *5*, 5−9.
(7) Guo, B.; Han, G. Y.; Li, M. Y.; Zhao, S. Z. Deposition of the Fractal-Like Gold Particles onto Electrospun Polymethylmethacrylate Fibrous Mats and Their Application in Surface-Enhanced Raman Scattering. *Thin Solid Films* **2010**, *518*, 3228−3233.
(8) Fan, M. K.; Andrade, G. F. S.; Brolo, A. G. A Review on the Fabrication of Substrates for Surface Enhanced Raman Spectroscopy and Their Applications in Analytical Chemistry. *Anal. Chim. Acta* **2011**, *693*, 7−25.
(9) Hao, E.; Schatz, G. C. Electromagnetic Fields around Silver Nanoparticles and Dimers. *J. Chem. Phys.* **2004**, *120*, 357−366.
(10) Canamares, M. V.; Garcia-Ramos, J. V.; Gomez-Varga, J. D.; Domingo, C.; Sanchez-Cortes, S. Comparative Study of the Morphology, Aggregation, Adherence to Glass, and Surface-Enhanced Raman Scattering Activity of Silver Nanoparticles Prepared by Chemical Reduction of Ag+ Using Citrate and Hydroxylamine. *Langmuir* **2005**, *21*, 8546−8553.
(11) Schmidt, M. S.; Hübner, J.; Boisen, A. Nanopillars: Large Area Fabrication of Leaning Silicon Nanopillars for Surface Enhanced Raman Spectroscopy. *Adv. Mater.* **2012**, *24*, OP10.
(12) Ou, F. S.; Hu, M.; Naumov, I.; Kim, A.; Wu, W.; Bratkovsky, A. M.; Li, X. M.; Williams, R. S.; Li, Z. Y. Hot-Spot Engineering in Polygonal Nanofinger Assemblies for Surface Enhanced Raman Spectroscopy. *Nano Lett.* **2011**, *11*, 2538−2542.
(13) Lim, D. K.; Jeon, K. S.; Kim, H. M.; Nam, J. M.; Suh, Y. D. Nanogap-Engineerable Raman-Active Nanodumbbells for Single-Molecule Detection. *Nat. Mater.* **2010**, *9*, 60−67.
(14) Dieringer, J. A.; Lettan, R. B.; Scheidt, K. A.; Van Duyne, R. P. A Frequency Domain Existence Proof of Single-Molecule Surface-Enhanced Raman Spectroscopy. *J. Am. Chem. Soc.* **2007**, *129*, 16249−16256.
(15) Ko, H.; Singamaneni, S.; Tsukruk, V. V. Nanostructured Surfaces and Assemblies as SERS Media. *Small* **2008**, *4*, 1576−1599.
(16) Alvarez-Puebla, R. A.; Agarwal, A.; Manna, P.; Khanal, B. P.; Aldeanueva-Potel, P.; Carbo-Argibay, E.; Pazos-Perez, N.; Vigderman, L.; Zubarev, E. R.; Kotov, N. A.; Liz-Marzan, L. M. Gold Nanorods 3d-Supercrystals as Surface Enhanced Raman Scattering Spectroscopy Substrates for the Rapid Detection of Scrambled Prions. *Proc. Natl. Acad. Sci. U.S.A.* **2011**, *108*, 8157−8161.
(17) Ko, H.; Chang, S.; Tsukruk, V. V. Porous Substrates for Label-Free Molecular Level Detection of Nonresonant Organic Molecules. *ACS Nano* **2009**, *3*, 181−188.
(18) Dzenis, Y. Spinning Continuous Fibers for Nanotechnology. *Science* **2004**, *304*, 1917−1919.
(19) Greiner, A.; Wendorff, J. H. Electrospinning: A Fascinating Method for the Preparation of Ultrathin Fibres. *Angew. Chem., Int. Ed.* **2007**, *46*, 5670−5703.
(20) Roskov, K. E.; Kozek, K. A.; Wu, W.-C.; Chhetri, R. K.; Oldenburg, A. L.; Spontak, R. J.; Tracy, J. B. Long-Range Alignment of Gold Nanorods in Electrospun Polymer Nano/Microfibers. *Langmuir* **2011**, *27*, 13965−13969.
(21) Zhou, Z.; Wu, X.-F.; Fong, H. Electrospun Carbon Nanofibers Surface-Grafted with Vapor-Grown Carbon Nanotubes as Hierarchical Electrodes for Supercapacitors. *Appl. Phys. Lett.* **2012**, *100*, 023115.
(22) Wang, Y.; Li, Y.; Yang, S.; Zhang, G.; An, D.; Wang, C.; Yang, Q.; Chen, X.; Jing, X.; Wei, Y. A Convenient Route to Polyvinyl Pyrrolidone/Silver Nanocomposite by Electrospinning. *Nanotechnology* **2006**, *17*, 3304.
(23) Dong, G. P.; Xiao, X. D.; Liu, X. F.; Qian, B.; Liao, Y.; Wang, C.; Chen, D. P.; Qiu, J. R. Functional Ag Porous Films Prepared by Electrospinning. *Appl. Surf. Sci.* **2009**, *255*, 7623−7626.
(24) He, D.; Hu, B.; Yao, Q.-F.; Wang, K.; Yu, S.-H. Large-Scale Synthesis of Flexible Free-Standing SERS Substrates with High Sensitivity: Electrospun PVA Nanofibers Embedded with Controlled Alignment of Silver Nanoparticles. *ACS Nano* **2009**, *3*, 3993−4002.
(25) Zhang, C.-L.; Lv, K.-P.; Cong, H.-P.; Yu, S.-H. Controlled Assemblies of Gold Nanorods in PVA Nanofiber Matrix as Flexible Free-Standing SERS Substrates by Electrospinning. *Small* **2012**, *8*, 648−653.
(26) Cao, M.; Cheng, S.; Zhou, X.; Tao, Z.; Yao, J.; Fan, L.-J. Preparation and Surface-Enhanced Raman Performance of Electrospun Poly(Vinyl Alcohol)/ High-Concentration-Gold Nanofibers. *J. Polym. Res.* **2012**, *19*, 9810.
(27) He, H.; Cai, W.; Lin, Y.; Dai, Z. Silver Porous Nanotube Built Three-Dimensional Films with Structural Tunability Based on the Nanofiber Template-Plasma Etching Strategy. *Langmuir* **2011**, *27*, 1551−1555.
(28) Lee, C. H.; Tian, L.; Abbas, A.; Kattumenu, R.; Singamaneni, S. Directed Assembly of Gold Nanorods Using Aligned Electrospun Polymer Nanofibers for Highly Efficient SERS Substrates. *Nanotechnology* **2012**, *4*, 275311.
(29) Zhang, C.-L.; Lv, K.-P.; Huang, H.-T.; Cong, H.-P.; Yu, S.-H. Co-assembly of Au Nanorods with Ag Nanowires within Polymer Nanofiber Matrix for Enhanced SERS Property by Electrospinning. *Nanoscale* **2012**, *4*, 5348−5355.
(30) Xie, X.; Yan, K.; An, Z.; Zhang, J. Facile Synthesis of Glass−Silver Nanodisk Core-Shell Composite Hollow Spheres. *RSC Adv.* **2012**, *2*, 5058−5061.
(31) Carlberg, B.; Ye, L. L.; Liu, J. H. Surface-Confined Synthesis of Silver Nanoparticle Composite Coating on Electrospun Polyimide Nanofibers. *Small* **2011**, *7*, 3057−3066.

(32) Jia, W. Z.; Wang, Y.; Basu, J.; Strout, T.; Carter, C. B.; Gokirmak, A.; Lei, Y. Nanoengineered Transparent, Free-Standing, Conductive Nanofibrous Membranes. *J. Phys. Chem. C* **2009**, *113*, 19525−19530.
(33) Sinha-Ray, S.; Zhang, Y.; Yarin, A. L. Thorny Devil Nanotextured Fibers: The Way to Cooling Rates on the Order of 1 kW/cm^2. *Langmuir* **2011**, *27*, 215−226.
(34) Guo, B.; Zhao, S. Z.; Han, G. Y.; Zhang, L. W. Continuous Thin Gold Films Electroless Deposited on Fibrous Mats of Polyacrylonitrile and Their Electrocatalytic Activity Towards the Oxidation of Methanol. *Electrochim. Acta* **2008**, *53*, 5174−5179.
(35) Ochanda, F.; Jones, W. E. Fabrication and Thermal Analysis of Submicron Silver Tubes Prepared from Electrospun Fiber Templates. *Langmuir* **2007**, *23*, 795−801.
(36) Bortolotto, L. *Direct Hydroxylation of Benzene to Phenol in a Microstructured Pd-Based Membrane Reactor*; KIT Scientific Publishing: Karlsruhe, Germany, 2011; p 59.
(37) Netzer, N. L.; Qiu, C.; Zhang, Y. Y.; Lin, C. K.; Zhang, L. F.; Fong, H.; Jiang, C. Y. Gold-Silver Bimetallic Porous Nanowires for Surface-Enhanced Raman Scattering. *Chem. Commun.* **2011**, *47*, 9606−9608.
(38) Zhang, L.; Luo, J.; Menkhaus, T. J.; Varadaraju, H.; Sun, Y.; Fong, H. Antimicrobial Nano-Fibrous Membranes Developed from Electrospun Polyacrylonitrile Nanofibers. *J. Membr. Sci.* **2011**, *369*, 499−505.
(39) Zhang, L. F.; Wang, X. X.; Zhao, Y.; Zhu, Z. T.; Fong, H. Electrospun Carbon Nano-Felt Surface-Attached with Pd Nanoparticles for Hydrogen Sensing Application. *Mater. Lett.* **2012**, *68*, 133−136.
(40) Ochanda, F.; Jones, W. E. Sub-Micrometer-Sized Metal Tubes from Electrospun Fiber Templates. *Langmuir* **2005**, *21*, 10791−10796.
(41) Park, H. K.; Yoon, J. K.; Kim, K. Novel Fabrication of Ag Thin Film on Glass for Efficient Surface-Enhanced Raman Scattering. *Langmuir* **2006**, *22*, 1626−1629.
(42) Chen, M.; Wang, L. Y.; Han, J. T.; Zhang, J. Y.; Li, Z. Y.; Qian, D. J. Preparation and Study of Polyacryamide-Stabilized Silver Nanoparticles through a One-Pot Process. *J. Phys. Chem. B* **2006**, *110*, 11224−11231.
(43) Tao, A.; Kim, F.; Hess, C.; Goldberger, J.; He, R.; Sun, Y.; Xia, Y.; Yang, P. Langmuir−Blodgett Silver Nanowire Monolayers for Molecular Sensing Using Surface-Enhanced Raman Spectroscopy. *Nano Lett.* **2003**, *3*, 1229−1233.
(44) Barakat, N. A. M.; Woo, K.-D.; Kanjwal, M. A.; Choi, K. E.; Khil, M. S.; Kim, H. Y. Surface Plasmon Resonances, Optical Properties, and Electrical Conductivity Thermal Hystersis of Silver Nanofibers Produced by the Electrospinning Technique. *Langmuir* **2008**, *24*, 11982−11987.
(45) Lee, C. H.; Tian, L.; Singamaneni, S. Paper-Based SERS Swab for Rapid Trace Detection on Real-World Surfaces. *ACS Appl. Mater. Interfaces* **2010**, *2*, 3429−3435.